Basic Science Liver

Subsets of innate lymphoid cells in acute liver injury

Alabbas, Saleh Y.[1, 2]; Movva, Ramya[2, 3]; Purdon, Amy S.[2]; Begun, Jakob[1, 2]; Florin, Timothy H.[1, 2]; Oancea, Iulia [1, 2]

1. Faculty of Medicine, University of Queensland, Brisbane, Queensland, Australia.
2. Chronic Disease Biology and Care, Mater Research Institute-University of Queensland, Brisbane, Queensland, Australia.
3. School of Pharmacy, Griffith University, Gold Coast, Queensland, Australia.

Introduction: Innate lymphoid cells (ILCs) are a recently described immune cell population that has been shown to mirror the phenotype and function of T cells without the requirement for antigen specificity. Specifically, ILCs are classified into three main groups based on the dominant transcription factor and the cytokines that they secrete. Group 1 ILCs secrete IFNγ and TNF; group 2 ILCs secrete IL-5, IL-9 and IL-13; and group 3 ILCs secrete IL-17A and IL-22. They have been linked to tissue repair and remodeling, and early responses against pathogens, and are associated with a number of autoimmune disorders. Thus, ILCs are considered to have an important role in inflammatory responses due to their secretion of important cytokines and interaction with components of the adaptive immune system. Various studies have suggested that different cytokines play an anti- or pro-inflammatory role following acute liver injury, outlining a potential role for ILCs in liver injury. In the gut, it has been suggested that NKp46^{+} ILC3 (IL-1710^{w} and IL-22^{high}) cells may play a protective role, whereas NKp46^{-}ILC3 (IL-17^{high} and IL-2210^{w}) cells may play a pathogenic role. We hypothesized that might be the case in liver pathology as well.

Methods: Four- to five-week-old C57BI/6 (wild type [WT]) mice were treated with either intraperitoneal vehicle control (water) or 500 mg APAP, to model acute liver injury. Mice were fasted overnight and feed was re-allowed immediately after APAP administration. They were sacrificed 24 hours after treatment. Tissues like liver and lamina propria isolated from small and large intestine were collected, and changes in the frequencies of ILC subsets were measured via flow cytometry (FACS). We also evaluated IL-17 and IL-22 cytokine production and measured a number of gene expressions associated with hepatic injury.

Results: APAP-treated WT mice had significant weight loss and hepatic inflammation at 24 hours, confirming the model of acute liver injury. FACS data from liver and lamina propria tissues revealed an expansion in ILC2 (about threefold) and ILC3 NKp46^{+} (about 15-fold) populations in APAP-treated mice at this time point. On the other hand, the frequency of ILC3 NKp46^{-} (about threefold) was decreased following liver injury in the same tissues as above.

Conclusion: At 24 hours after liver injury, a time point associated with a significant anti-inflammatory component, we have shown an expansion of anti-inflammatory and a decrease of pro-inflammatory ILC populations. This suggests an associated role of ILCs in hepatic injury. We are further exploring ILC functions with cytokine production in the absence of T cells and how this anti-/pro-inflammatory balance changes with time.

Iron blocks the secretion of apolipoprotein E in cultured human adipocytes

Britton LJ[1,2,3,4], Bridle K[1,2], Jaskowski LA[1,2], He J[4], Ng C[5], Ruelcke JE[6], Reiling J[1,2,7], Santrampurwala N[1], Hill MM[8], Whitehead JP[5], Subramaniam VN[9], Crawford DHG[1,2]

1. Gallipoli Medical Research Institute, Brisbane, Queensland, Australia
2. School of Medicine, University of Queensland, Brisbane, Queensland, Australia
3. Department of Gastroenterology, Princess Alexandra Hospital, Brisbane, Queensland, Australia
4. Mater Research Institute, Brisbane, Queensland, Australia
5. School of Life Sciences, University of Lincoln, Lincoln, UK
6. Translational Research Institute, Brisbane, Queensland, Australia
7. Department of Surgery, NUTRIM School of Nutrition and Translational Research in Metabolism, Maastricht University, Maastricht, The Netherlands
8. QIMR Berghofer Medical Research Institute, Brisbane, Queensland, Australia
9. Institute of Health and Biomedical Innovation and School of Biomedical Sciences, Queensland University of Technology, Brisbane, Queensland, Australia

Introduction: Adipose tissue dysfunction plays a central role in the pathogenesis of non-alcoholic steatohepatitis (NASH) through the dysregulation of adipokines and the generation of insulin resistance. Recent data support a role for iron in the regulation of adipose tissue function. The effects of iron on the secretome of adipocytes have not been established.

Methods: We treated human adipocytes (Simpson–Golabi–Behmel syndrome adipocytes—differentiated *in vitro*) with 0, 25, 100, and 500 uM iron, as ferric ammonium citrate, for 48 hours. We found that treatment with 100 uM iron caused significant increases in intracellular iron concentration, but did not alter proliferation or total protein secretion from these cells. To determine if iron modulated

the secretion of specific proteins from the adipocyte secretome, we performed quantitative proteomics using SILAC (stable isotope labeling with amino acids in cell culture), followed by tandem mass spectrometry.

Results: A total of 339 proteins were quantified from the adipocyte secretome, of which 59 were differentially secreted in response to iron, with a more than twofold change and *P* value < 0.05. We validated the iron-induced down-regulation of apolipoprotein E (ApoE) by western blotting, with a reduction of 67% (*P* = 0.001) and 76% (*P* = 0.007) by SILAC and western blot, respectively. Conversely, cell lysate samples demonstrated a greater than 11-fold increase in intracellular ApoE in response to iron (*P* = 0.0005), without a significant change in ApoE mRNA levels. The ratio of secreted ApoE to cell lysate ApoE was reduced by 98% by iron (*P* = 0.002).

Conclusion: These findings indicate that cellular iron loading blocks ApoE secretion, causing ApoE to become sequestered within adipocytes. ApoE has been shown to have a protective role in promoting adipocyte hyperplasia over hypertrophy and also protects against diet-induced steatohepatitis in mice. The interaction between iron and ApoE in adipocytes may represent a novel therapeutic target for treating humans with NASH.

Liver oxidative stress, apoptosis, and autophagy are increased in a mouse model of iron overload

ACG Chua,[1] A Domenichini,[1] RD Delima,[1] C Elsegood,[1] JK Olynyk,[2] D Trinder[1]

[1]School of Medicine, University of Western Australia, Perth, Western Australia, Australia, [2]Department of Gastroenterology, Fiona Stanley Hospital, Perth, Western Australia, Australia.

Introduction: Hereditary hemochromatosis (HH) is a common primary iron overload disorder caused by mutations in *HFE* or *TFR2* genes, which may cause liver iron overload and liver fibrosis, cirrhosis, and hepatocellular carcinoma. Secondary liver iron overload can also develop from excess dietary iron intake. The aim of this study was to examine the role of iron overload in the development of liver injury by examining oxidative stress, apoptosis, and autophagy in mouse models of primary (HH) and secondary (dietary iron supplementation) iron overload.

Methods: HH mice with disrupted *HFE* and *TFR2* genes and wild-type (WT) mice were fed a control iron diet (0.01%) until they reached 13 or 26 weeks of age. Other HH and WT mice were fed an iron-supplemented diet (2% carbonyl iron) from 10 weeks of age for 3 weeks. Liver iron concentration (LIC) was measured by inductively coupled plasma mass spectrometry, and liver injury was assessed by measurement of serum alanine transaminase activity. Oxidative stress was determined by measurement of lipid peroxidation (malondialdehyde) and antioxidant enzymes heme oxygenase 1, and copper and manganese superoxide dismutase protein expression. Apoptosis was evaluated by Tunel, and mRNA and protein expression of apoptosis and autophagy markers were determined by polymerase chain reaction and western blot, respectively.

Results: LIC was increased in HH mice at 13 weeks (HH, 137 ± 6 *vs* WT, 20 ± 1 μmol/g; $P < 0.001$) and was further raised at 26 weeks of age (HH, 168 ± 12 *vs* WT, 27 ± 2 μmol/g; $P < 0.001$). Dietary iron supplementation increased LIC in WT mice to similar levels observed in HH mice fed a control iron diet (137 ± 8 μmol/g), and in HH mice, levels were elevated markedly (245 ± 5 μmol/g; $P < 0.001$). Serum alanine transaminase activity was raised in HH mice at both ages ($P < 0.01$), but levels did not change with dietary iron loading. Malondialdehyde levels were increased in HH ($P < 0.01$) and dietary iron-loaded WT mice ($P < 0.05$), but levels did not change significantly with age. Antioxidant enzyme heme oxygenase protein levels were increased in HH ($P < 0.01$) and dietary iron-loaded WT mice ($P < 0.001$) and were further augmented by 1.7-fold in dietary iron-loaded HH mice. In contrast, both copper and manganese superoxide dismutase protein levels were reduced in HH mice ($P < 0.01$) and dietary iron-loaded WT mice ($P < 0.01$), with an additional decline by 30%–50% in dietary iron-loaded HH mice. Apoptosis was evident in dietary iron-loaded HH mice by Tunel. Furthermore, expression of pro-apoptotic proteins Bid and Bak were significantly upregulated in HH ($P < 0.01$) and dietary iron-loaded HH mice ($P < 0.05$), while anti-apoptotic Bcl-xl mRNA expression was reduced in HH mice ($P < 0.05$) at 26 weeks. Protein expression of autophagy proteins LC3II and Atg3 were raised in HH mice at both ages ($P < 0.05$), but dietary iron loading did not enhance expression further in HH mice.

Conclusions: Iron-induced liver injury was observed in mouse models of primary and secondary iron overload. There was hepatic oxidative stress with increased lipid peroxidation and changes in antioxidant enzyme expression in both models, while apoptosis and autophagy were both evident in HH mice, suggesting they contribute to liver injury processes in iron overload disease.

Circulatory microRNA-365a-3p as a potential biomarker for the diagnosis of pediatric cystic fibrosis-associated liver disease

Diego A. Calvopina[1], Miranda A. Coleman[1], Manuel A. Fernandez-Rojo[1], Leesa F. Wockner[2], Cameron J. McDonald[3], Peter J. Lewindon[1,4,5], Grant A. Ramm[1,5]

[1]Hepatic Fibrosis Group, QIMR Berghofer Medical Research Institute, Brisbane, Queensland, Australia; [2]QIMR Berghofer Statistics Unit, QIMR Berghofer Medical Research Institute, Brisbane, Queensland, Australia; [3]Membrane Transport Group, QIMR Berghofer Medical Research Institute, Brisbane, Queensland, Australia; [4]Department of Gastroenterology and Hepatology, Lady Cilento Children's Hospital, Brisbane, Queensland, Australia; [5]Faculty of Medicine and Biomedical Sciences, University of Queensland, Brisbane, Queensland, Australia.

Introduction: In Australia, cystic fibrosis (CF) affects one out of 2500 newborns, of whom 15%–20% develop severe liver abnormalities and 5% die due to end-stage liver disease. CF is an autosomal recessive disorder that affects the CF transmembrane regulator channel expressed in cholangiocytes and the gall bladder. As a consequence of decreased bile flow, thickened secretions block the bile ducts and lead to hepatic and cholangiocyte injury, characteristics of CF-associated liver disease (CFLD). CFLD is one of the leading non-respiratory causes of morbidity and mortality in children with CF. Liver biopsy, an invasive procedure, remains the gold standard to assess the severity of liver damage in CFLD before the advent of cirrhosis and portal hypertension. We investigated circulatory microRNAs (miRNAs) as non-invasive biomarkers to diagnose and assess disease progression of pediatric CFLD.

Methods: Our study assessed the circulating miRNA signature of 90 children allocated into three study cohorts based on clinical, biochemical, and imaging assessment, as follows: healthy controls (controls, $n = 30$); CF patients with no evidence of liver disease (CFnoLD, $n = 30$); and CFLD ($n = 30$; sub-divided according to liver biopsy fibrosis stages: F0, F1–2 and F3–4; $n = 10$ each). Serum miRNAs were analyzed using the Ion Torrent sequencing platform. Sequencing libraries were created by pooling 10 samples per group. Significant differentially expressed miRNAs were detected using normalized read counts and pair-wise comparisons. Selected miRNAs were further validated in 124 individual samples by quantitative real-time polymerase chain reaction and analyzed using ANOVA ($P < 0.05$).

Results: We identified let-7g-5p, miR-34a-5p, miR-122–5p, miR-365a-3p, miR-18a-5p, miR-126–5p, and miR-142–3p to be significant differentially expressed between all three study groups. Post-hoc analysis showed the upregulation of miR-34a-5p ($P = 0.0042$), miR-122–5p ($P = 0.0015$), and miR-365a-3p ($P = 0.0002$), while let-7g-5p ($P = 0.0034$) and miR-142–3p ($P = 0.0047$) were downregulated in CFLD patients compared with CFnoLD patients. ROC curve analysis was used to determine the ability of these miRNAs to differentially diagnose liver disease in children with CF. miR-365a-3p showed the best predictive value, with an area under the curve (AUC) of 0.745 ($P = 0.0001$; sensitivity, 70.4%; specificity, 67.5%). Additionally, let-7g-5p with an AUC of 0.708 ($P = 0.0010$; sensitivity, 70.4%; specificity, 65%), miR-34a-5p with an AUC of 0.707 ($P = 0.0014$; sensitivity, 71.4%; specificity, 64.1%) and miR-122–5p with an AUC of 0.708 ($P = 0.0010$; sensitivity, 70.4%; specificity, 62.5%) were also capable of differentiating between CFLD and CFnoLD. In contrast, miR-18a-5p was significantly upregulated in both CFnoLD and CFLD compared with controls ($P < 0.0001$), with a predictive value of AUC = 0.822 ($P < 0.0001$; sensitivity, 80%; specificity, 80%), suggesting an important role in CF.

Conclusion: Although diagnostic panels using combinations of these miRNAs require validation in larger cohorts, our study has identified several serum miRNAs with potential to diagnose liver disease in children with CF.

Alagebrium inhibits progression of non-alcoholic fatty liver disease to steatohepatitis and liver fibrosis by blocking AGE/RAGE pathway in mice

HKDH Fernando[1], DIG Rajapaksha[1], PW Angus[1, 2], CB Herath[1]
[1]Department of Medicine, University of Melbourne, Austin Health, Melbourne, Victoria, Australia.
[2]Department of Gastroenterology and Hepatology, Austin Health, Melbourne, Victoria, Australia.

Introduction: Non-alcoholic fatty liver disease (NAFLD) affects up to 30% of the adult population and is now a major cause of liver disease-related premature illness and death in Australia. There is currently no established drug therapy, and treatment is largely based on lifestyle modification, which is difficult to achieve in most patients. Advanced glycation end products (AGEs), formed as a result of non-enzymatic reaction between reducing-sugars and proteins, lipids or nucleic acids and which works through their receptor, RAGE (receptor for advanced glycation end products), have been implicated as a second hit that drives NAFLD to steatohepatitis and liver fibrosis. Therefore, in this study, we investigated the therapeutic potential of the AGE crosslink breaker alagebrium (Ala) in mice fed a high-fat, high-cholesterol (HFHC) diet or HFHC baked (HFb) diet to increase dietary AGE exposure.

Methods: Six-week-old male C57Bl/6 mice were fed an HFHC diet for 40 weeks. A second group of mice was fed the HFb diet (baked 1 hour at 160°C) to increase dietary AGE levels. A third group of mice, which was fed on the HFb diet, was treated with Ala (10 mg/kg body weight) by daily oral gavage for the last 10 weeks of the experiment. The content of N(6)-(carboxymethyl)lysine (CML), the best characterized AGE type, in HFHC and HFb was measured by gas chromatography mass spectrometry. At 40 weeks, animals were sacrificed, and blood and liver tissue were harvested. Liver function tests were determined in plasma. Gene expression of RAGE, profibrotic and proinflammatory cytokines, and hepatic stellate cell (HSC) activation marker was determined by quantitative polymerase chain reaction. Hepatic fibrosis was quantified by picrosirius red staining, and therapeutic effects of Ala were tested in mice fed a high AGE diet.

Results: CML levels were threefold higher in HFb than in HFHC pellets. Long-term consumption of the HFHC diet produced steatosis, steatohepatitis, and fibrosis after 40 weeks. Alanine aminotransferase (ALT) and alkaline phosphatase (ALP) levels were higher ($P < 0.01$) in mice fed the HFb diet compared with those of HFHC-fed mice. However, Ala treatment significantly reduced ALT ($P < 0.001$) and ALP ($P < 0.01$) in HFb-fed mice, suggesting that Ala improved hepatocellular damage. The increased liver RAGE expression ($P < 0.001$) in mice fed the HFb diet was abrogated ($P < 0.001$) by Ala treatment. Moreover, Ala significantly ($P < 0.05$) downregulated the gene expression of inflammatory cytokines, monocyte chemoattractant protein-1 and tumor necrosis factor-α and HSC activation marker, α-smooth muscle actin in mice fed the HFb diet. Furthermore, the HFb diet caused increased ($P < 0.001$) expression of profibrotic cytokine, transforming growth factor-β1 (TGF-β1) and extracellular matrix (ECM) gene collagen I in the liver. Moreover, Ala treatment reduced the increased expression of TGF-β1 and collagen I by more than 50% ($P < 0.01$) in the livers of HFb-fed mice. Gene expression changes of proinflammatory and profibrotic cytokines were accompanied by increased ($P < 0.05$) ECM deposition in mice fed the HFb diet, leading to liver fibrosis. Interestingly, Ala treatment strongly inhibited liver fibrosis in mice fed the HFb diet, restoring it to that seen in HFHC-fed mice.

Conclusion: The progression of NAFLD to steatohepatitis and liver fibrosis is triggered by activation of RAGE with elevated AGE content in the diet. We conclude that activation of AGE/RAGE pathway may serve as a second hit that drives simple steatosis to steatohepatitis and fibrosis. Moreover, we show that the AGE crosslink breaker alagebrium inhibits the activation of the AGE/RAGE pathway in NAFLD and, thus, has potential to be used as a treatment for fibrosis associated with NAFLD.

Evolution of the renin angiotensin system in a rat model of non-cirrhotic portal hypertension

LS Gunarathne[1], DIG Rajapaksha[1], HKDH Fernando[1], PW Angus[1, 2], CB Herath[1]
[1]Department of Medicine, University of Melbourne, Austin Health, Melbourne, Victoria, Australia.
[2]Department of Gastroenterology and Hepatology, Austin Health, Melbourne, Victoria, Australia.

Aim: The rat model of partial portal vein ligation (PPVL) has been widely used in studies investigating pathophysiology of non-cirrhotic portal hypertension (PH). However, the contribution of the renin angiotensin system (RAS) in the development of PH following PPVL remains largely unknown. Therefore, this time course study investigated the evolution of RAS gene expression in three closely related vascular beds, namely, the mesenteric, gut and liver vasculatures, during the development of PH in PPVL rats.

Methods: Six-week-old Sprague Dawley rats were randomly allocated into six groups (n = 6). In rats undergoing PPVL surgery, a calibrated stenosis in the portal vein was created using a 19G needle (OD, 1.067 ± 0.0005). Sham-operated rats served as controls. On Days 1, 2, 5, 10, and 14 after PPVL, the portal vein of anesthetized rats was cannulated through an ileocolic vein with a PE-10 catheter, which was connected to a highly sensitive pressure transducer for continuous monitoring of portal pressure (PP). PP in sham-operated rats was measured 14 days after surgery. Fifteen minutes after continuous PP recording, rats were sacrificed for sample collection. Gene expression of RAS components. including angiotensin converting enzyme (ACE), ACE2, Mas receptor (MasR), angiotensin II type 1 receptor (AT1R), and angiotensin II type 2 receptor (AT2R), was determined in second and third order mesenteric vessels, jejunum and liver tissues by quantitative polymerase chain reaction (qPCR).

Results: PPVL significantly (P < 0.0005) increased PP from a mean (± SD) of 5.25 ± 0.91 mmHg in sham-operated rats to more than 12 mmHg (12.4 ± 0.99) in PPVL rats and was dropped to about 10 mmHg (10.6 ± 0.12) after Day 5. A drop in pressure is consistent with the establishment of collateral circulation in this model. qPCR analysis showed jejunal AT1R expression was downregulated (P < 0.005) by more than sixfold from Day 1 to about threefold at Day 14 after PPVL, whereas ACE2 expression tended to be increased. Consistent with AT1R expression in the gut, mesenteric vascular AT1R was also downregulated (P < 0.0005) by more than sixfold. We found that in this vasculature, both AT2R (P < 0.05) and ACE2 (P < 0.0005) were also downregulated in PPVL rats compared with sham-operated controls. In contrast, AT1R expression in the liver was upregulated from Day 2 after PPVL compared with the controls. Moreover, liver ACE, ACE2, and MasR were upregulated by more than 10-fold at Day 2 of PPVL rats compared with the controls.

Conclusion: The gut is the first to respond to portal vein obstruction to the blood flow with decreased AT1R expression, leading to inhibition of angiotensin II-mediated vasoconstriction, which allows more blood to flow through the vasculature. This in turn may allow adequate gut perfusion. The mesenteric vasculature also responds by blocking vasoconstriction pathway mediated by angiotensin II, thus allowing adequate gut perfusion. A decrease in the expression of vasodilatory components of the RAS, ACE2 and AT2R, in the mesenteric vasculature may help in maintaining the gut perfusion without exacerbating the vasodilatation. Increased liver ACE2, which may increase vasodilatory Ang(1–7)

production, and together with increased MasR, is likely to be a counter-regulatory mechanism in response to increased angiotensin II-mediated vasoconstriction. We conclude that development of non-cirrhotic PH may result from decreased angiotensin II-mediated vasoconstriction in the gut and mesenteric vascular beds.

New murine model for hepatocellular carcinoma

Henderson J.M. [1], Polak N. [1], Chen J.B. [1], McCaughan G.W. [1,2], Kench J.G. [1], Roediger B. [1], Bachovchin W.W. [3], Gorrell M.D. [1]

1. Centenary Institute and Sydney Medical School, University of Sydney, Sydney, New South Wales, Australia.

3. Tufts University, Boston, Massachusetts, USA.

Introduction: Hepatocellular carcinoma (HCC) is responsible for more than 70% of primary liver cancer and is the second leading cause of cancer-related deaths worldwide. Due to the ineffectiveness of current therapies, HCC patients have a 16% 5-year survival rate. HCC models typically involve an initial insult of *N*-nitrosodiethylamine (DEN), followed by the long-term administration of either a pro-fibrotic or pro-steatotic insult. The major drawback of this approach is the time taken for HCC to appear (8–12 months). Here we show that combining pro-steatotic and pro-fibrotic insults can produce HCC in 6 months. Liver fibrosis is predominantly driven by activated hepatic stellate cells (HSCs). Following liver insult, HSCs undergo activation from a quiescent vitamin A-storing cell to a proliferative, myofibroblast-like, alpha smooth muscle actin (SMA)-expressing cell exhibiting upregulated collagen synthesis, as well as increased expression of fibroblast activation protein (FAP). FAP activity is very low in resting tissues but is highly induced during inflammation and upregulated in carcinoma-associated fibroblasts (CAFs) of most human tumors.

Method: Mice were injected with DEN at 12 days of age and treated from weaning with thioacetamide (TAA) or both TAA and a high-fat diet (HFD). Histological measurement of inflammation, steatosis, and fibrosis used hematoxylin and eosin staining. Alpha-SMA and F4/80 were assessed by immunohistochemistry. Flow cytometry was carried out when tumors were large, at 36 weeks of age. Statistics used non-parametric *t*-test and ANOVA. Quantitative real-time polymerase chain reaction was performed on 93 genes.

Results: The incidence of HCC was greater in the DEN–TAA–HFD-treated mice (83%) than the DEN–TAA-treated mice (20%) at 24 weeks of age ($n = 5–6$). DEN–TAA–HFD treatment showed increased fibrosis and inflammatory cell aggregation compared with control, and increased steatosis compared with both DEN–TAA and control at 24 weeks ($n = 5–6$, *t*-test; $P < 0.05$, $P < 0.001$, respectively). The number of dysplastic lesions in DEN–TAA–HFD-treated mice (25 lesions) was greater than in DEN–TAA mice (14 lesions) ($n = 5–6$). Alpha-SMA (% positive area/total tissue area) expression increased in both the DEN–TAA–HFD livers and the DEN–TAA livers compared with control ($n = 5–6$, *t*-test: $P < 0.05$, $P < 0.01$, respectively). Flow cytometry analysis of tumors and surrounding liver tissue from DEN–TAA–HFD mice, compared with non-diseased liver showed a decrease in $CD45^+CD90^+$ and a decrease in $CD45^+CD19^+$ populations inside the tumors and surrounding tissue compared with control ($P < 0.0001$). By polymerase chain reaction, 34 transcripts were differentially expressed in DEN–TAA–HFD liver ($P < 0.05$), including upregulation of the macrophage-associated genes CD163, Nos2, CD47, CD64, CD68 and Keap1 and the cell growth-associated genes Bc12-L1 and IGF-1. CD136 mRNA was downregulated in DEN–TAA–HFD liver. Myofibroblasts in DEN–TAA–HFD-treated mice at 36 weeks of age were targeted with 3996, a FAP activated bortezomib-like prodrug. Flow cytometry using the fluorescent FAP inhibitor 4613b

showed that the intrahepatic CD45$^-$CD29+FAP+ population of myofibroblasts decreased in 3996-treated mice.

Conclusion: This new DEN–TAA–HFD model provides a more rapid means of examining HCC and potential therapies.

Characterising and combating the immune modulatory and epithelial-to-mesenchymal plasticity properties of hepatocellular carcinoma-derived cancer stem cells

Aparna Jayachandran[1,2], Ritu Shrestha[1,2], Haolu Wang[2,3], Prashanth Prithviraj[4], Bijay Dhungel[1,2], I-Tao Huang[1,2] and Jason C Steel[1,2].

[1]Liver Cancer Unit, Gallipoli Medical Research Institute, Greenslopes Private Hospital, Brisbane, Queensland, Australia
[2]Faculty of Medicine, University of Queensland, Brisbane, Queensland, Australia
[3]Translational Research Institute, Brisbane, Queensland, Australia
[4]Olivia Newton John Cancer Research Centre, Melbourne, Victoria, Australia

Background: Hepatocellular carcinoma (HCC) is the fastest increasing cause of cancer mortality in Australia despite the development of various therapeutic strategies. The development of an effective immunotherapy for HCC has proven difficult, with the induction of anticancer-directed immune responses seldom resulting in complete tumor eradication. Understanding the mechanisms by which cancer cells are able to escape host immune responses is critical for the development of successful immunotherapeutic treatments. Cancer stem cells (CSCs) represent a specialized population of transformed cells distinct from the majority of "differentiated" tumor cells. These cells are responsible for tumor initiation, organization and maintenance and play a major role in the resistance to radiation and chemotherapy. Recently, epithelial-to-mesenchymal plasticity (EMP) that enables tumor metastasis has emerged as an important regulator of CSC immune modulation. Despite the importance of CSCs, very little is known about the sensitivity of these cells to immune surveillance and immune killing in HCC.

Hypothesis and Aims: Our hypothesis is that, to successfully form and maintain tumors, CSCs must suppress or avoid host immune responses, and that EMP is closely associated with CSC immune modulation. The aim of this study is to enrich and purify CSCs from human and murine HCC cell lines and to examine the relationship between immune modulatory and EMP properties of CSCs.

Methods and Results: In this study, using a modified sphere-forming serum-free culture system, we enriched stem-like cells from a panel of 20 human- and mouse-derived HCC cell lines. We assessed their stemness characteristics by evaluating the mRNA and protein levels of stemness genes and a cell surface stem cell marker. We imaged the CSCs *in vivo* with high-resolution multiphoton fluorescence lifetime imaging. Subsequently, we analyzed the immune-modulating characteristics of the CSCs using quantitative reverse transcription polymerase chain reaction (qRT-PCR), flow cytometry and ELISA. We identified immune modulatory

pathways, including MHC-I down regulation and TGF-β and IL-10 upregulation, that CSCs may use to suppress immune recognition. Next, we show evidence that CSCs with immunosuppressive characteristics are closely linked with an EMP phenotype and function assessed by qRT-PCR, immunofluorescence staining and motility assays. To examine the clinical relevance of our findings, we analyzed HCC patient datasets available from the Cancer Genome Atlas and found that the expression of immune modulatory and EMP markers resulted in worse overall survival (hazard ratio [HR], 1.7; 95% CI, 1.24–2.44; *P* = 0.001) and recurrence-free survival (HR, 1.67; 95% CI, 1.16–2.41; *P* = 0.005).

Conclusions: Our study demonstrated that the HCC CSCs exhibit distinctive immune modulatory and EMP markers that can be potentially used as biomarkers to stratify patients with HCC. The insights gained from this research may open new avenues to design immunotherapy strategies to treat HCC by specifically targeting CSC populations.

Lipid droplet homeostasis is crucial for the establishment of polarity in collagen sandwich culture of rat hepatocytes

Sun Woo Sophie Kang[1,3], Victoria Cogger[1,2], David Le Couteur[1,2] and Dong Fu[3,4]

1. Ageing and Alzheimers Institute, ANZAC Research Institute, Concord Clinical School and Sydney Medical School, Sydney, New South Wales, Australia.
2. Charles Perkins Centre, University of Sydney, Sydney, New South Wales, Australia.
3. Faculty of Pharmacy, University of Sydney, Sydney, New South Wales, Australia.
4. UNC Eshelman School of Pharmacy, University of North Carolina, Chapel Hill, North Carolina, USA.

Introduction: Hepatocyte polarization is an energy-dependent process that is crucial for the cellular function and viability. Our previous study has demonstrated that fatty acid β-oxidation and oxidative phosphorylation (OXPHOS) in mitochondria is an important energy source for establishment of polarity in hepatocytes, and lipid droplets are likely a crucial endogenous resource in providing fatty acids. However, it is unclear how lipid droplet homeostasis is regulated during the establishment of hepatocyte polarization. Therefore, the current study investigates multiple events involved in lipid droplet homeostasis, including lipolysis, lipophagy, *de novo* fatty acid synthesis and cholesterol esterification, and how they contribute to supplying fatty acid for β-oxidation and OXPHOS during hepatocyte polarization.

Methods: After pharmacological inhibition of these cellular events involved in lipid droplet homeostasis, amounts of lipid droplets were quantified, and fatty acid levels, ATP production and polarization were analyzed.

Results: Increased lipid droplet staining and upregulated expressions of perilipin 2, a lipid droplet surface-associated protein known to regulate lipid droplet size and accumulation, revealed that there was an increase in lipid droplet accumulation within hepatocytes when lipolysis was inhibited. Consequently, intracellular fatty acid levels and expressions of fatty acid binding protein 1, a protein involved in intracellular fatty acid trafficking, significantly decreased. As a result, ATP production was significantly impaired, leading to inhibition of polarization. These results indicate that lipolysis is the driving force in mobilizing fatty acids from lipid droplets for polarization. Conversely, there was a significant reduction in the amount of lipid droplets and perilipin 2 expressions when autophagy was inhibited, suggesting autophagy is involved in lipid droplet formation instead of the breakdown of lipid droplets to generate fatty acids. In addition, fatty acid levels and ATP levels decreased and polarization was impaired after inhibition of autophagy, demonstrating autophagy-mediated lipid droplet formation is critical for polarization. We further confirmed this in starved hepatocytes, where there was an increase in the amount of lipid droplets, together with upregulation of autophagy. Besides autophagy-mediated formation of lipid droplets, other cellular mechanisms, such as *de novo* fatty acid synthesis and cholesterol esterification, also caused impairment to the growth

of lipid droplets. Significant downregulation of perilipin 2 was accompanied by reduction in fatty acid levels and ATP levels, which subsequently caused inhibition of polarization. Thus, maintenance of lipid droplet homeostasis requires contributions from multiple pathways.
Conclusion: Our findings show that hepatocytes use multiple pathways to regulate lipid droplet homeostasis, which provides adequate fatty acids for ATP production during the establishment of polarization. These pathways include lipolysis-mediated generation of fatty acids, and formation of lipid droplet via autophagy, as well as *de novo* fatty acid synthesis and cholesterol esterification.

Human amnion epithelial cells reduce liver fibrosis and macrophage infiltration in a "fast-food diet" model of non-alcoholic steatohepatitis

Nathan Kuk[1,2], Alexander Hodge[1,2], Ying Sun[1,2], Jeanne Correia[1,2], Majid Alhomrani[1,2,3], Rebecca Lim[3], Gregory Moore[1,2], William Sievert[1,2]

[1] Centre for Inflammatory Disease, Monash University, Melbourne, Victoria, Australia

[2] Gastroenterology and Hepatology Unit, Monash Health, Melbourne, Victoria, Australia

[3] Hudson Institute of Medical Research, Melbourne, Victoria, Australia

Introduction: Non-alcoholic steatohepatitis (NASH) is associated with the metabolic syndrome and can lead to liver cirrhosis and hepatocellular carcinoma. Currently, there are no effective treatments except lifestyle modifications. Sourced from human placentas, human amnion epithelial cells (hAEC) and hAEC-conditioned media (hAEC-CM) possess anti-inflammatory and anti-fibrotic properties. We examined the efficacy of these cells in a diet-induced NASH model.

Methods: C57BL/6J mice received a "fast-food" diet (21% fat, 2% cholesterol, with 42 g/L fructose drinking water). At Week 34, Group 1 (*n* = 17) and Group 2 (*n* = 17) received an intraperitoneal injection of 2×10^6 hAECs. Group 3 (*n* = 17) received thrice-weekly injections of 400 µL hAEC-CM for 8 weeks. At Week 38, Group 2 received an additional injection of 2×10^6 hAECs. Controls were untreated. All mice were culled at Week 42. Liver collagen deposition and hepatic stellate cell activation were determined by Sirius red staining and alpha-smooth muscle actin (-SMA) immunohistochemistry. Computer-assisted morphometry was used to quantify the percentage of positively stained liver (expressed as percentage area of liver tissue). Fibrosis regulation was evaluated with immunofluorescence microscopy for the transforming growth factor (TGF)-β-regulated protein phosphorylated SMAD 2/3 (pSMAD2/3). Matrix metalloproteinase 9 (MMP-9) was measured using quantitative polymerase chain reaction. Liver inflammation was measured through serum alanine aminotransferase and macrophage staining

(F4/80+). Metabolic parameters such as total cholesterol, glucose tolerance, and body weight were also assessed.

Results: Control mice receiving the fast-food diet demonstrated peri-cellular hepatic fibrosis and steatosis typical of NASH. Compared with controls, liver fibrosis area was reduced in all hAEC- and hAEC-CM-treated mice by 40% ($P < 0.0001$). Similarly, treatment reduced the number of activated stellate cells by 43% ($P < 0.0001$) and pSMAD 2/3 signaling by 45% ($P < 0.001$). hAECs also increased MMP-9 expression twofold ($P < 0.05$). The hepatic macrophage population was lowered by 47% ($P < 0.0001$) (Figure 1). hAEC and hAEC-CM treatment did not significantly alter metabolic parameters such as body weight, total cholesterol, or glucose tolerance.

Conclusion: hAECs and hAEC-CM reduce liver fibrosis and macrophage infiltration in a fast-food diet-induced murine model of non-alcoholic fatty liver disease through reduced stellate cell activation, reduced TGF-β signaling, increased matrix metalloproteinase expression, and decreased macrophage numbers. Although hAECs and hAEC-CM do not affect the metabolic components of NASH, their therapeutic potential is promising and warrants further investigation.

Figure 1 Treatment effects of hAEC and hAEC-CM on NASH

Novel mechanistic imaging biomarkers for early prediction of acetaminophen-induced hepatotoxicity

X. Liang[1], H. Wang[1], X. Liu[1], M. Touraud[2], J.B. Chouane[2], B. Tse[3], M.S. Roberts[1]

[1]*Therapeutics Research Centre*, *University of Queensland Diamantina Institute*, *University of Queensland*, *Brisbane, Queensland, Australia*;
[2]*Department of Pharmacy*, *University of Rennes 1*, *Rennes, France*;
[3]*Translational Research Institute*, *Brisbane*, *Queensland*, *Australia*.

Introduction: Acetaminophen (APAP) is a widely used over-the-counter analgesic and antipyretic drug. However, its toxicity is the foremost cause of liver injury in the Western world. Currently, no adequate biomarkers are available for guiding treatment, resulting in patients being undertreated or overtreated with a time-consuming and potentially harmful antidote. Alterations in liver microperfusion play an important role in the development of APAP-induced liver injury and are directly involved in disease pathogenesis. Here, we applied contrast enhanced ultrasonography (CEU) with a photoacoustic imaging system for monitoring the changes in hepatic microvascular perfusion as novel mechanistic imaging biomarkers for APAP-induced livery injury.

Methods: After infusion of microbubble contrast agent, these bubbles were collapsed in the liver and post-bubble destruction refilling was measured in the liver. Local perfusion was monitored *in vivo* in mice after APAP poisoning and treatment. Hepatic perfusion was quantified using a destruction–replenishment model, and perfusion parameters were calculated using customized software including relative blood flow (rBF) and mean transit time (mTT).

Results: We found that APAP overdose significantly decreased hepatic perfusion at the early time points (within 2 hours), where mTT started to increase and rBF decreased from 2 hours after APAP overdose. In the meantime, oxygen saturation in liver parenchyma significantly decreased, to 62%, compared with control liver of over 80%. After NAC treatment for 12 hours, all of these parameters of hepatic perfusion were improved compared with the untreated group, and these changes correlated well with conventional biochemical and histological assessments.

Conclusion: CEU with a photoacoustic imaging system can non-invasively monitor the changes in liver microvascular perfusion as novel mechanistic imaging markers for APAP-induced livery

injury in mice, allowing precise structural and functional assessments of injury and the efficacy of treatment. This novel technique can be translated to clinical use in humans.

Hepatospheres formed in quasi-spherical microwells to study the therapeutic efficacy of novel liver-targeted iron chelator-loaded nanoformulations

Tianqing (Michelle) Liu[1*], Shanshan Guo[1,2], Guangjun Nie[2], Gregory J Anderson[1]

[1] Iron Metabolism Laboratory, QIMR Berghofer Medical Research Institute, Brisbane, Queensland, Australia
[2] CAS Key Laboratory for Biomedical Effects of Nanomaterials and Nanosafety, National Center for Nanoscience and Technology of China, Beijing, China

Hepatocyte-based *in vitro* culture models are widely used to study liver metabolism and drug uptake. However, conventional two-dimensional monolayer hepatocyte cultures do not closely recapitulate liver-specific functions and morphological properties.[1] Hepatospheres have been recognized as a better *in vitro* liver model for drug screening and toxicity studies. Here, quasi-spherical microwells (spheriwells) were fabricated using an ice lithographic bench-top microfabrication strategy.[2] The concave microwells prepared enabled the formation of dense and homogeneous hepatospheres that we have used as a model to study targeted nano-therapy.

Significant pathology accompanies body iron accumulation in iron loading disorders such as thalassemia, and therapy involves the chemical removal of iron using iron chelators. Current chelator treatments remain suboptimal. Clinically, desferrioxamine is the most effective iron binding compound with the most favorable safety profile, but an onerous parenteral administration regimen means that patient compliance is low. We have developed chelator-loaded polymeric nanoparticles (NPs) that specifically target hepatocytes, cells particularly prone to iron loading, using galactose as a targeting ligand for the asialoglycoprotein receptor. Uptake of targeted NPs into three-dimensional hepatospheres was studied by confocal microscopy. Higher accumulation of galactose-NPs was observed compared with non-targeted nanoparticles. This nanoparticle-based chelating system could potentially benefit patients suffering from iron overloading disorders.

References

1 Swift B, Pfeifer ND, Brouwer KLR. Sandwich-cultured hepatocytes: an in vitro model to evaluate hepatobiliary transporter-based drug interactions and hepatotoxicity. *Drug Metab. Rev.* 2010; 42: 446–71.
2 Liu T, Winter M, Thierry B. Quasi-spherical microwells on superhydrophobic substrates for long term culture of multicellular spheroids and high throughput assays. *Biomaterials* 2014; 35: 6060–8.

Hepatocyte EphA2 signaling is important for the development of liver fibrosis and the ductular reaction in a murine model of chronic liver disease

M Melino[1], G Miller[2], AW Boyd[1], B Day[1], P Bertolino[3], AD Clouston[2], KPA MacDonald[1]

[1]QIMR Berghofer Medical Research Institute, Brisbane, Queensland, Australia [2] Envoi Specialist Pathologists, Brisbane, Queensland, Australia [3] Centenary Institute and AW Morrow Gastroenterology and Liver Centre, University of Sydney and Royal Prince Alfred Hospital, Sydney, New South Wales, Australia.

Introduction: The Eph receptors are the largest subfamily of receptor tyrosine kinases and have been increasingly implicated in inflammation and tissue repair after injury. In particular, the Eph receptor EphA2 is known to be upregulated by established mediators of liver fibrosis such as lipopolysaccharide and pro-inflammatory cytokines including IL-1 [17]. Using the thioacetamide (TAA) model of chronic liver disease, we identify a role for EphA2 in fibrotic progression and demonstrate that blocking this pathway ameliorates liver fibrosis.

Methods: Microarray analysis implicated a rapid induction of the Eph/ephrin signaling pathway, specifically EphA2, in whole livers isolated from TAA-treated C57BL/6 wild-type (WT) mice. EphA2 mRNA and protein expression was confirmed in total liver, hepatocyte, and mononuclear cell populations from naive and TAA-treated WT mice. Liver fibrosis, SMA^{+} myofibroblasts and the ductular reaction were assessed in WT, $EphA2^{-/-}$ and EphA4-Fc treated TAA mice.

Results: Quantitative polymerase chain reaction (Figure 1A) and immunohistochemistry (Figure 1B) analyses confirmed an upregulation of EphA2 following 1 week of TAA treatment and identified hepatocytes as the major EphA2 expressing cells following liver injury. $EphA2^{-/-}$ mice demonstrated reduced liver fibrosis (Figure 2A) and SMA^{+} myofibroblasts in comparison to WT following 1 week of TAA treatment. After 6 weeks of TAA, in addition to reduced fibrosis, $EphA2^{-/-}$ mice displayed reduced ductular reaction in association with decreased hepatic progenitor cell (HPC) numbers and the HPC mitogen, TWEAK (Figure 2B–D). Notably, inflammatory cell populations (monocytes, neutrophils, T and B cells) were comparable in WT and $EphA2^{-/-}$ livers despite the reduction in fibrosis, suggesting EphA2 involvement occurs downstream of the initial inflammatory response. Finally, to determine the feasibility of Eph signaling blockade for the treatment of liver fibrosis, after 3 weeks of TAA treatment, WT mice were co-administered with the broad Eph receptor inhibitor, EphA4-Fc. Livers from mice receiving the EphA4-Fc construct demonstrated reduced fibrosis in association with a significant decrease in HPC numbers.

Conclusion: EphA2 is crucial for the development of liver fibrosis and the ductular reaction and represents a novel targetable pathway for the treatment of chronic liver disease.

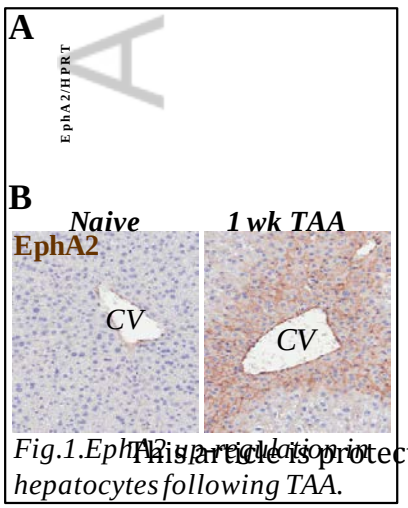

Fig.1.EphA2 upregulation in hepatocytes following TAA.

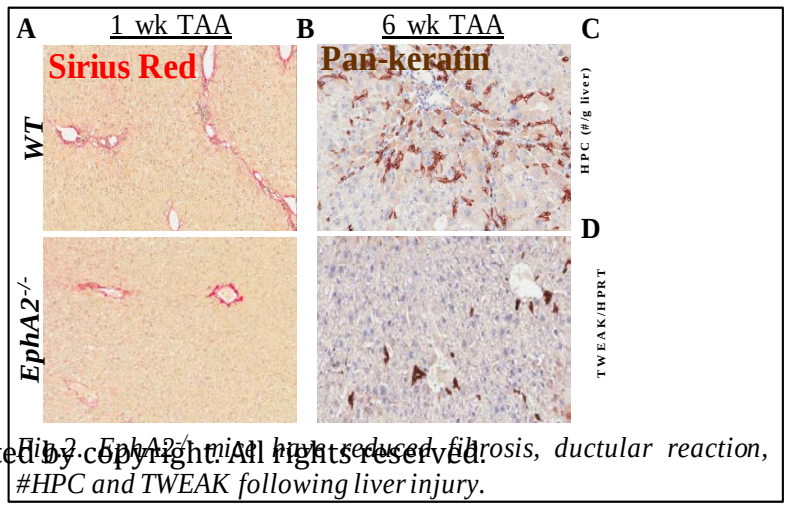

Fig.2. EphA2-/- mice have reduced fibrosis, ductular reaction, #HPC and TWEAK following liver injury.

Fasting increases hepatic hepcidin expression and can overcome the effect of *Hfe* deletion in mice

C.S.G. Mirciov[1,2], S.J. Wilkins[1], G.J. Anderson[1,2], D.M. Frazer[1].
[1]QIMR Berghofer Medical Research Institute, Brisbane, Queensland, Australia.
[2]University of Queensland, Brisbane, Queensland, Australia.

Introduction: Several prominent disorders, such as hereditary hemochromatosis and β-thalassemia, are associated with the inappropriately low expression of the iron regulatory hormone hepcidin (encoded by the *Hamp1* gene). Pharmaceutical agents that increase hepcidin production would, therefore, be of benefit in these conditions. A recent study has demonstrated that fasting can increase hepcidin production in mice, although the potential effects of circadian variations in *Hamp1* expression were not taken into account. We have examined the effect of fasting in more detail to determine whether the pathway(s) responsible might provide novel targets for pharmaceutical intervention in disorders of iron homeostasis.
Methods: C57BL/6 mice were fasted for 5, 10, 16, and 24 hours before euthanasia, then blood and tissue samples were collected for analysis. The effect of a 16-hour fast was also examined in mice maintained on an iron-deficient diet for 6 weeks, mice injected with erythropoietin, and *Hfe* knockout mice (a model of hereditary hemochromatosis). Tissue collection was performed at the same time of day for all experiments to avoid the potential effects of circadian variations in hepcidin production. The expression of hepatic *Hamp1*, *bone morphogenetic protein 6* (*Bmp6*) and *cAMP responsive element binding protein 3-like 3* (*Creb313*), and bone marrow *erythroferrone* was determined by real-time quantitative polymerase chain reaction. Serum iron levels and liver iron concentration were determined using colorimetric assays.
Results: We have confirmed that fasting increases hepatic *Hamp1* expression in mice, with maximal expression seen after 16 hours (2.3-fold). This was despite a significant decrease in serum iron levels and an increase in bone marrow *erythroferrone* expression, although a significant increase in *Bmp6* expression (1.4-fold) was observed in mice fasted for 16 hours. *Hamp1* expression was increased in both iron-deficient fasting mice and in fasted mice treated with erythropoietin, but in neither case was this increase statistically significant. Surprisingly, fasting of *Hfe* knockout mice resulted in a 7.7-fold increase in *Hamp1* expression when compared with unfasted knockout mice, and a 3.7-fold increase when compared with unfasted wild-type mice. No significant change in *Bmp6* expression was seen when fasted *Hfe* knockout mice were compared with non-fasted animals. Significant increases in hepatic *Creb313* were observed in all fasted mice.
Conclusion: These studies have confirmed that fasting increases the expression of hepatic *Hamp1* in mice. Although the effect of fasting was not able to overcome the stimuli to decrease *Hamp1* expression in chronically iron-deficient mice or following erythropoietin injection, fasted *Hfe* knockout animals expressed higher levels of *Hamp1* than both unfasted *Hfe* knockout and wild-type mice. This indicates that the induction of *Hamp1* expression in response to fasting is independent of *Hfe*. Our data also suggest that the effect is independent of changes to serum iron levels, *erythroferrone* expression or *Bmp6* production. *Creb313* encodes a transcription factor known to bind the *Hamp1* promotor and its induction in all fasting conditions studied supports previous suggestions that hepcidin production is regulated by gluconeogenic signals. Our results suggest that targeting the pathway(s) involved in the

regulation of hepcidin production by fasting could be of clinical benefit in conditions such as hemochromatosis and β-thalassemia.

IL-17RB signaling is a critical contributor to hepatotoxin-induced liver fibrosis

Nalkurthi BC[1], Melino M[1], Miller G[2], Le Texier L[1], Lineburg K[1], Teal B[1], Clouston A[2, 3], MacDonald KPA[1]

[1]QIMR Berghofer Medical Research Institute, Brisbane, Queensland, Australia.[2] Envoi Specialist Pathologists, Brisbane, Queensland, Australia.[3] Centre for Liver Disease Research, University of Queensland, Brisbane, Queensland, Australia.

Introduction: IL-17RB signaling is emerging as a key mediator in various inflammatory and mucosal disease settings. The IL-17RB receptor subunit is required for IL-17B and IL-17E (IL-25) signaling. The role of IL-17E in chronic inflammatory disease, including liver fibrosis, is controversial, with reports of both pathogenic and regulatory functions. Moreover, the role of IL-17B in liver fibrosis remains unexplored. We therefore investigated the role of IL-17RB signaling in liver fibrosis.

Methods: Liver fibrosis was induced in C57BL/6.WT and B6.IL-17RB$^{-/-}$mice by oral administration of thioacetamide (TAA; 300 mg/L) for 1, 6, and 12 weeks. Collagen deposition was measured by Sirius red staining and collagen 1A gene expression. Monocyte infiltration (F4/80), smooth muscle activation (anti-SMA), and ductular reaction (DR-(CK-WSS)) were assessed by immunohistochemistry. Fibrogenic, cellular, and soluble immune mediators were assessed and quantified by quantitative polymerase chain reaction, cytokine bead array, and flow cytometry.

Results: Livers from mice deficient in IL-17RB (IL-17RB$^{-/-}$) displayed significantly reduced fibrosis after 1, 6, and 12 weeks of TAA administration. At 1 week, livers from IL-17RB$^{-/-}$mice exhibited about a 50% reduction in CCL2 levels and a significant decrease in peri-central monocytic infiltration and myofibroblast activation compared with WT mice. Notably, the administration of IL-17E, but not IL-17B, to naïve mice (5 □g/day for 4 days) indued elevated circulating and liver CCL2 levels, with associated monocytic infiltration, collagen deposition, and myofibroblast activation. In response to TAA administration in WT mice, CCL2 expression was induced in liver macrophages, monocytes, and eosinophils. Strikingly, CCL2 produced from macrophages and eosinophils, but not monocytes, was IL-17RB dependent, explaining the only partial reduction in IL-17RB$^{-/-}$mice. Although direct signaling of IL-17E in eosinophils has been reported, IL-17RB mRNA expression profiling demonstrated a 10- and 30-fold increase in IL-17RB expression in hepatocytes compared with liver-associated myeloid cells in steady state and following TAA administration, respectively. During fibrotic progression (6–12-week TAA treatment), abrogated fibrosis in IL-17RB$^{-/-}$mice was associated with significantly decreased levels of the hepatic progenitor cell mitogen, TWEAK, and a significantly reduced DR.

Conclusion: Our data demonstrate that IL-17RB signaling is required for the initiation and progression of hepatotoxin-induced liver fibrosis. The IL-17RB ligand IL-17E contributes to elevated CCL2 levels following TAA treatment through the induction of CCL2 expression from macrophages and eosinophils. As we recently reported the CCL2 deficiency only partially attenuated fibrosis in this model, these data, together with the high levels of IL-17RB expression on hepatocytes, suggest additional mechanisms are operating. The contribution of hepatocyte IL-17RB signaling to fibrosis is currently under investigation.

Experimental hepatocellular carcinoma treated with dipeptidyl peptidase-4 inhibition, metformin, or anti-PD1

Authors: Natasa Polak, Stephanie Wetzel, James M. Henderson, Geoffrey W. McCaughan and Mark D. Gorrell
Presenting Author: Natasa Polak, PhD
Affiliations: Centenary Institute and Sydney Medical School, University of Sydney, Sydney, New South Wales, Australia, and AW Morrow Gastroenterology and Liver Centre, Royal Prince Alfred Hospital, Sydney, New South Wales, Australia.

Background: Hepatocellular carcinoma (HCC) is a primary liver malignancy that generally develops from chronic liver injury causing scarring known as cirrhosis. Sorafenib is a kinase inhibitor drug that is in clinical use to treat HCC. 1G244 is a potent and selective inhibitor of dipeptidyl peptidase (DPP)-8 and DPP-9 that stimulates the immune system and can induce macrophage pyroptosis. A new immune cell targeted drug class that blocks PD-1 is used to shrink some lung and skin cancers, but has not been evaluated in HCC. The antidiabetic drugs sitagliptin and metformin exhibit anti-tumor effects via DPP-4 inhibition and AMPK activation, respectively. Reported here are the preliminary results of such treatments in a novel primary HCC mouse model.
Aims: To use a novel mouse model of HCC to investigate various agents in primary liver cancer.
Methods: Liver from 24-week-old male mice (C57BL/6J) was analyzed following diethyl nitrosamine (DEN) at age 12 days then high-fat diet (HFD) and the hepatotoxin thioacetamide (TAA) in the drinking water from 4 to 24 weeks of age. A potentially therapeutic intervention, or its control procedure, was provided to each mouse for the final 4 weeks. These interventions were: (1) antibody to PD-1 (10 mg/kg intraperitoneal) twice a week, and isotype control; and (2) 1G244 (1 mg/kg, 2×/day) and/or sorafenib (50 mg/kg, 3×/week via gavage). Other mice were provided metformin (200 mg/L drinking water) and/or sitagliptin (32 mg/kg) for 14 weeks, from 10 weeks of age. Lesions, encompassing small cell change, focal fatty change, dysplasia, HCC, cholangiocarcinoma, and necrosis, were counted on hematoxylin and eosin stained sections. The statistic used was the Mann–Whitney one-tailed *t*-test.
Results: All mice had developed HCC at 24 weeks of age. The total numbers of lesions in both mice treated with sorafenib ($P = 0.019$) and with sorafenib plus 1G244 ($P = 0.031$) were fewer than their controls (Figure 1). In contrast, anti-PD-1-treated mice had more lesions ($P = 0.04$; Figure 1) and more dysplastic lesions ($P = 0.016$) than their controls. Sitagliptin plus metformin in a prevention protocol significantly decreased the total number of liver lesions ($P = 0.005$). Number of dysplastic/tumor spots visible on the liver surface was similar between all groups. Blood glucose levels, steatosis, and fibrosis were similarly elevated in all groups of mice. There were no significant differences in HCC, liver or spleen weights, or the other observed parameters.
Conclusion: Dysplasia but not HCC was reduced by sorafenib and by sitagliptin combined with metformin. Neither dysplasia nor HCC were reduced by anti-PD1.

Figure 1 Number of lesions by treatment group

Angiotensin converting enzyme 2–adeno-associated viral vector gene therapy ameliorates liver fibrosis in diabetic mice with non-alcoholic fatty liver disease

DIG Rajapaksha[1], LS Gunarathne[1], S Andrikopoulos[1], PW Angus[1,2], CB Herath[1]
[1]*Department of Medicine*, *University of Melbourne*, *Austin Health*, *Melbourne, Victoria*, *Australia*.
[2]*Department of Gastroenterology and Hepatology*, *Austin Health*, *Melbourne, Victoria*, *Australia*.

Introduction: Non-alcoholic fatty liver disease (NAFLD) is recognized as the most common cause for chronic liver disease in developed countries, including Australia, whereas it is emerging as a major health problem in other parts of the world. NAFLD is frequently associated with obesity and diabetes. However, there is no specific therapy to treat this condition. We have recently shown that liver-specific adeno-associated viral (AAV) vector-carrying angiotensin converting enzyme 2 (ACE2) markedly reduced steatohepatitis in a short-term mouse model fed with a methionine-choline deficient diet.[1] ACE2 is the major enzyme of the alternate axis of the renin–angiotensin system that generates antifibrotic peptide angiotensin-(1–7) from profibrotic peptide, angiotensin II. The aim of this study was to investigate the antifibrotic effect of ACE2 therapy in a long-term dietary NAFLD model with diabetes.
Methods: C57BL/6 mice were fed a high-fat, high-cholesterol (HFHC) diet for 40 weeks to induce NAFLD. They were rendered diabetic by two consecutive daily injections of streptozotocin (STZ) after 15 weeks of HFHC diet. A single intraperitoneal injection of ACE2–AAV or a control vector carrying human serum albumin (HAS–AAV) was administered to mice 15 weeks after STZ injection, and the animals were sacrificed 10 weeks after ACE2 therapy. Hepatic fibrosis was determined using picrosirius red staining. ACE2, profibrotic and pro-inflammatory gene expressions were determined using quantitative polymerase chain reaction. Liver biochemistry and serum creatinine, cholesterol, triglyceride, high-density lipoprotein, and glucose levels were determined.
Results: ACE2 therapy increased hepatic ACE2 gene expression by 75-fold ($P < 0.01$) compared with the control vector-injected group. ACE2 therapy improved hepatocellular damage, as reflected by significantly ($P < 0.05$) reduced alanine aminotransferase and aspartate aminotransferase levels compared with control vector-treated mice. ACE2 also reduced serum creatinine ($P < 0.01$) and glucose ($P < 0.05$) levels. Moreover, ACE2 therapy significantly ($P < 0.05$) downregulated pro-inflammatory IL-6 and MCP-1 gene expressions in diabetic mice compared with the control vector-treated mice. These changes were associated with a significant ($P < 0.05$) reduction in the activation of hepatic stellate cells, as reflected by reduced αSMA expression, leading to a significant reduction in the expression of profibrotic cytokines, TGF-β1 and CTGF, and matrix component collagen 1. Thus, profound reduction in pro-

inflammatory and profibrotic cytokine, and matrix gene expression in ACE2-treated mice has led to a significant reduction ($P < 0.05$) in hepatic fibrosis in diabetic NAFLD mice compared with that in the control vector-injected mice. In addition, serum cholesterol and triglyceride levels were dramatically reduced ($P < 0.05$) in ACE2-treated mice compared with the control vector-injected animals.

Conclusion: ACE2 gene therapy significantly improves liver fibrosis in NAFLD mice with diabetes. Importantly, this gene therapy has major implications in diabetic patients with liver disease, as diabetes is known to exacerbate liver injury. We therefore conclude that ACE2 gene therapy has potential as a therapy for NAFLD patients with diabetes.

References

1. Mak KY, Chin R, Cunningham SC, et al. ACE2 therapy using adeno-associated viral vector inhibits liver fibrosis in mice. *Mol. Ther.* 2015; 23: 1434–43.

Do macrophages play a role in the development of endotoxin-induced biliary injury in rats?

Reiling J,[1,2,3,4] Bridle KB,[1,2] Schaap FG,[4] Jaskowski L,[1,2] Santrampurwala N,[1,2] Britton LJ,[1,2,5] Campbell CM,[6] Olde Damink SWM,[4,7] Crawford DHG,[1,2] Dejong CHC,[4,8] Fawcett J [1,2,3,9]

[1]Faculty of Medicine, University of Queensland, Brisbane, Queensland, Australia, [2]Gallipoli Medical Research Institute, Brisbane, Queensland, Australia, [3]PA Research Foundation, Brisbane, Queensland, Australia, [4]Department of Surgery, NUTRIM School of Nutrition and Translational Research in Metabolism, Maastricht University, Maastricht, The Netherlands, [5]Department of Gastroenterology, Princess Alexandra Hospital, Brisbane, Queensland, Australia, [6]Envoi Specialist Pathologists, Brisbane, Queensland, Australia [7]Department of Surgery, RWTH Universitätsklinikum, Aachen, Germany, [9]Queensland Liver Transplant Service, Princess Alexandra Hospital, Brisbane, Queensland, Australia

Introduction: It has previously been shown that exposure to endotoxins, in the form of lipopolysaccharides (LPSs), results in prompt and severe injury to the bile ducts. The exact mechanism by which this injury develops remains unclear. We hypothesized that hepatic macrophages play an important role in the development of endotoxin-induced biliary injury and that no injury would occur in their absence.

Methods: Groups of rats were pre-treated for 48 hours with clodronate liposomes (n = 24) and compared with animals that did not receive liposomes (n = 24). Pre-treatment was followed by sham operation, administration of LPSs, or a combination of LPSs and 30 minutes of warm hepatic ischemia (IRI+LPS). After 6 hours of reperfusion, blood, bile, and liver tissue was collected for further analysis. Injury to the small bile ducts was assessed, serum liver tests were performed, and bile composition was evaluated. The permeability of the blood–biliary barrier (BBB) was assessed using horseradish peroxidase (HRP). In short, 2000 IU of HRP was injected in the inferior vena cava and bile was collected for a period of 10 minutes. The output of HRP in bile was subsequently measured using a colorimetric assay.

Results: Hepatic macrophages were successfully depleted from the rat livers by clodronate pre-treatment (–90%, $P < 0.001$). Macrophage depletion could not, however, prevent the development of severe small bile duct injury in four animals (50%) of the clodronate+IRI+LPS group and six animals (75%) of the clodronate+LPS group. Furthermore, BBB impairment persisted, as evidenced by leakage of HRP in bile in both LPS-treated groups. Endotoxin-induced elevation of the chemokine Mcp-1 in bile was unaffected by macrophage depletion.

Conclusions: Depletion of macrophages did not prevent development of biliary injury following LPS or LPS-enhanced IRI. Cholangiocyte rather than macrophage activation may underlie this injury.

A novel assay for studying the hepcidin–ferroportin axis and its application in characterizing a new *SLC40A1* mutation

Daniel F. Wallace[1,2], Cameron J. McDonald[2], Lesa Ostini[2], David Iser[3], Annabel Tuckfield[4], V. Nathan Subramaniam[1,2]

[1]Institute of Health and Biomedical Innovation and School of Biomedical Sciences, Queensland University of Technology, Brisbane, Queensland, Australia; [2]Membrane Transport Laboratory, QIMR Berghofer Medical Research Institute, Brisbane, Queensland, Australia; [3]Department of Gastroenterology, St Vincent's Hospital, Melbourne, Victoria, Australia; [4]Royal Melbourne Hospital, Melbourne, Victoria, Australia.

Background and Aims: The hepcidin–ferroportin axis underlies the pathophysiology of many iron-associated disorders. The clinical presentation and treatment of ferroportin disease is highly dependent on the functional consequences of the causative mutation: transport-deficient or hepcidin-resistant. The aims of this study were to identify the molecular basis of disease in a patient with iron overload, and to use a novel antibody, which we developed, to characterize ferroportin variants and their sensitivity to hepcidin.

Methods: Targeted next-generation sequencing using an iron metabolism gene panel developed in our group was used to identify variants in a patient with iron overload. Antibodies against the largest extracellular loop of ferroportin were characterized by western blotting, immunofluorescence, and flow cytometry. Wild-type and mutant ferroportin constructs, transfected into HEK293 cells, were analyzed. The effects on hepcidin-mediated internalization and iron transport were studied using a novel flow cytometry-based assay.

Results: We identified a novel ferroportin variant (p.D84E) associated with iron overload. An antibody specific for cell surface ferroportin was characterized and a novel flow cytometry-based assay was developed, which measures the dynamics of hepcidin-mediated ferroportin internalization, and can accurately and efficiently characterize the functional consequences of ferroportin mutations. Using this assay, we showed that this ferroportin variant is unable to transport iron, and is also insensitive to hepcidin-mediated internalization.

Conclusion: The p.D84E mutation results in the classical form of ferroportin disease and is predicted to affect a key residue involved in ferroportin function, resulting in an inability to transport iron. Our novel ferroportin antibody and flow cytometry assay will be a valuable tool

for investigating the dynamics of ferroportin trafficking, response to hepcidin or other agonists/antagonists, and structure-function relationships.

Characterizing and predicting the *in vivo* kinetics of mesenchymal stem cells and their secretome for the treatment of liver cirrhosis

Haolu Wang[1], Xiaowen Liang[1], Liesbeth Weijs[2], Anastasia Brooks[3], Xin Liu[1], Michael S. Roberts[1], Darrell H.G. Crawford[4]

[1]Therapeutics Research Centre, University of Queensland Diamantina Institute, University of Queensland, Brisbane, Queensland, Australia

[2]Queensland Alliance for Environmental Health Sciences, University of Queensland, Brisbane, Queensland, Australia

[3]School of Biomedical Sciences, University of Queensland, Brisbane, Queensland, Australia

[4]School of Clinical Medicine, University of Queensland, Brisbane, Queensland, Australia

Presenting Author: Haolu Wang

Introduction: Mesenchymal stem cells (MSCs) and the immunomodulatory cytokines produced by MSCs have considerable potential for the treatment of liver cirrhosis. However, the success of MSC-based therapy has been grossly impeded by the poorly understood cell–tissue interactions and ill-defined cell pharmacokinetics in the body.

Methods: The mouse organ disposition and cell–tissue interactions of green fluorescent protein-expressing MSCs after intravenous injection were first visualized by high-resolution intravital microscopy. The concentration–time profiles of the administered MSCs in the liver were elucidated using flow cytometry. Based on these findings, the physiologically based kinetic model was developed for the *in vivo* kinetics of therapeutic MSCs, and the two-compartment pharmacokinetic model was developed for MSC secretome (Figure 1). The utility of these models was examined across species and administration routes by extrapolation of this model to rats and humans, as well as to intrahepatic arterial injection. The clinical application of this model was also tested with data obtained from stem cell-based therapies given to patients with liver cirrhosis in two clinical trials.

Results: Our model successfully characterized the *in vivo* kinetics of therapeutic MSCs and their secretome (interleukin 6 and interleukin 8). Sensitivity analysis revealed that the targeting efficiency of therapeutic MSCs is determined by the lung retention and interaction between MSCs and the liver, including cell arrest, depletion, and release. Model validations with multiple external datasets indicated its accurate inter-route and inter-species predictive capability in both normal state and liver cirrhosis.

Conclusion: Our models accurately characterized and predicted the *in vivo* kinetics of therapeutic MSCs and their secretome. They provide the optimized dosage, route of administration, and targeting strategies for MSC-based therapy for liver cirrhosis, to design standardized treatment protocols.

Figure 1

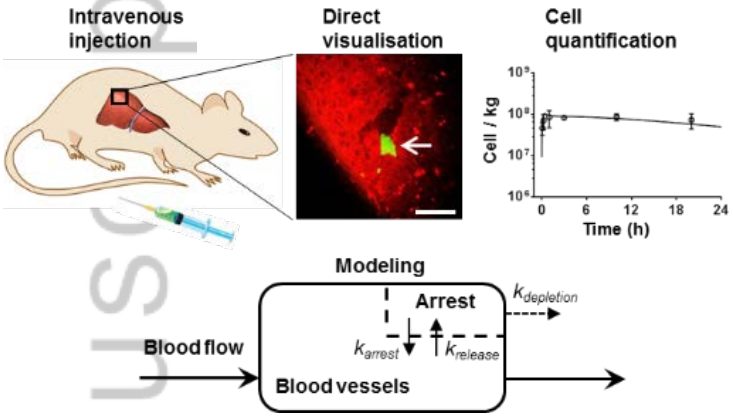

Serum microRNAs as biomarkers for cirrhosis and hepatocellular carcinoma in hepatitis C: Preliminary results and future potential

Anna Weis,[1,2] Grant A Ramm,[1,2] Louise Marquart,[3] Lachlan Webb,[3] David Smith,[3] Leesa Wockner,[3] Isabell Hoffmann,[3,4] Richard Skoien[1,2,5]

[1]Hepatic Fibrosis Group, QIMR Berghofer Medical Research Institute, Brisbane; [2]Faculty of Medicine, University of Queensland, Brisbane; [3]QIMR Berghofer Statistics Unit, QIMR Berghofer Medical Research Institute, Brisbane, Queensland, Australia; [4]Institute of Medical Biostatistics, Epidemiology and Informatics, University Medical Centre, Johannes Gutenberg University of Mainz, Mainz, Germany; [5]Department of Gastroenterology and Hepatology, Royal Brisbane and Women's Hospital, Brisbane, Queensland, Australia

Background: Despite improved treatments, cirrhosis related to chronic hepatitis C (CHC) remains an enormous public health burden. Identification of patients at highest risk of cirrhosis-related complications and the earlier diagnosis of hepatocellular carcinoma (HCC) remain unmet clinical needs. The gold standard for the diagnosis of cirrhosis or HCC remains liver biopsy, which is invasive, prone to sampling error and does not reflect the dynamic nature of chronic liver disease. Dynamic imaging in HCC can be inconclusive, and the currently accepted tumor marker (alpha-fetoprotein) is suboptimal in its sensitivity and specificity, and dynamic, meaning diagnosis and treatment is delayed in many cases. The roles of microRNAs in the progression of liver disease are being elucidated, and their potential to act as biomarkers in HCC is being explored.

Methods: Based on expert clinical assessment, transient elastography and/or medical imaging, 60 patients with CHC were subdivided into three study cohorts: mild to moderate disease (F0–2; $n = 20$); cirrhosis (F4; $n = 20$); and cirrhosis with HCC (HCC; $n = 20$). A quantitative reverse transcription–polymerase chain reaction (qRT-PCR) microarray (Liver miFinder PCR Array; Qiagen) was used to assess the expression levels of 372 liver-related microRNAs in serum. The differential expression of microRNAs across all cohorts was measured using quantile normalization and the modified *t*-test ($P < 0.05$). Eight of the most differentially expressed microRNAs on the microarray were selected for further validation within the same study cohort using an independent qRT-PCR approach (Exiqon miRCURY LNA miRNA qRT-PCR kit). Significant differences in microRNA expression between cohorts were detected using ANOVA and Tukeys post-hoc pair-wise comparison ($P < 0.05$).

Results: The qRT-PCR microarray demonstrated differential expression for at least 10 microRNAs across the cohorts of patients with mild disease *versus* cirrhosis *versus* HCC. The validation study of eight of these confirmed significantly increased expression of microRNA-22-3p ($P = 0.0397$) and microRNA-409-3p ($P = 0.0405$) in patients with cirrhosis *versus* mild disease (F0–2). When patients with HCC were compared with those with cirrhosis alone, expression levels of microRNA-122-5p ($P = 0.0010$) and microRNA-151a-5p ($P = 0.0499$) were significantly lower, whereas microRNA-486-5p expression ($P = 0.0018$) was significantly increased.

Conclusion: This study identifies and validates the differential expression of several microRNAs across the spectrum of disease severity due to CHC. Preliminary results suggest microRNA-122-5p, microRNA-

486-5p, microRNA-151a-5p, microRNA-22-3p, and microRNA-409-3p have potential as biomarkers for the diagnosis of cirrhosis and/or HCC. The expression levels of candidate microRNAs, particularly microRNA-486-5p, in atypical or early HCC are now being investigated. Ongoing studies are also being undertaken to identify microRNAs that are associated with disease progression and cirrhosis-related complications.

Smoking worsens the fibrosis of alcoholic chronic pancreatitis via activation of pancreatic stellate cells

Zhihong Xu[1,2], Srinivasa P. Pothula[1,2], Alexandra T.K. Lee[1,2], Danny Tran[1,2], Stephen J. Pandol[3], Romano C. Pirola[1,2], Jeremy S. Wilson[1,2] and Minoti V. Apte[1,2]

[1]*Pancreatic Research Group*, *South Western Sydney Clinical School*, *Faculty of Medicine*, *University of New South Wales, Sydney, New South Wales, Australia*.

[2]*Ingham Institute for Applied Medical Research*, *Sydney*, *New South Wales*, *Australia*.

[3]*Cedars Sinai Medical Center*, *Los Angeles*, *California, USA*.

Background: Epidemiological studies indicate that smoking accelerates the progression of alcoholic chronic pancreatitis (AP), as evidenced by earlier development of calcification and fibrosis. However, the mechanisms mediating these effects are unknown. Activated pancreatic stellate cells (PSCs) are the key cells responsible for producing the fibrosis of AP. We have recently shown that PSCs express nicotinic acetylcholine receptors (nAChRs) that bind the ligands nicotine and nicotine-derived nitrosamine ketone (NNK). Thus, we hypothesize that smoke compounds, in combination with ethanol, activate PSCs, leading to enhanced fibrosis of the gland.

Aims: To assess: 1) the effects of cigarette smoke exposure on the extent of necroinflammation and fibrosis in a rat model of AP; and 2) the *in vitro* effects of smoke compounds ± alcohol on rat PSC proliferation in the presence and absence of the nAChR antagonist mecamylamine. In addition, PSC migration and endoplasmic reticulum (ER) stress in PSCs was measured.

Methods: 1) SD rats fed Lieber-DeCarli alcohol diets for 11 weeks were challenged with LPS (3 mg/kg; weekly intravenous injection) or saline in Weeks 9, 10, and 11. Rats were housed either conventionally (exposed to room air) or in a custom-designed smoke exposure chamber and, from Week 5 to Week 11, exposed to cigarette smoke, at a level equivalent to heavy smoking (25 cigarettes/day). Hence, there were five groups (n = 3 rats/group): control (C); alcohol + saline (A); alcohol + LPS (AL); alcohol + smoke + saline (AS); and alcohol + smoke + LPS (ASL). Hematoxylin and eosin sections were scored for injury (oedema, acinar necrosis, inflammation); Sirius red sections were assessed morphometrically for collagen deposition. Immunohistochemistry for myeloperoxidase (MPO) was performed to assess inflammatory cell infiltration. Acinar cell apoptosis was determined by TUNEL staining.

2) Rat PSCs were exposed to cigarette smoke extract (CSE, 40 µg/mL) or NNK (100 mM) ± ethanol (E, 10 mM) for 48 hours in the presence and absence of mecamylamine (500 µM), and cell proliferation was assessed. PSC migration was determined using fluorescence labeling. ER stress in PSCs was measured using spliced XBP-1 as an ER stress marker.

Results: Data are expressed as mean ± SEM.

1) Results from the animal model are shown in Figure 1.

2) CSE and NNK, alone and in combination with ethanol, significantly increased PSC proliferation (% of control: CSE, 128.9 ± 1.5*; NNK, 127.6 ± 1.6*; CSE + E, 130.2 ± 2.3*; NNK + E, 119.3 ± 4.0; *$P < 0.05$ *vs* control $n = 4$/group). This induction was abolished in the presence of mecamylamine. PSC migration was significantly increased by CSE, NNK, CSE + E, or NNK + E (% of control: CSE, 210 ± 29.5*; NNK, 150 ± 13*; CSE + E, 211 ± 17.5*; NNK + E, 206 ± 15.7*; *$P < 0.05$ *vs* control $n = 5$/group). Messenger RNA expression of spliced XBP-1 was significantly increased by CSE, NNK, or CSE + E (% of control: CSE, 142 ± 3.7*; NNK, 158.1 ± 8.2*; CSE + E, 149.3 ± 5.2*; *$P < 0.05$ *vs* control $n = 5$/group).

Conclusions: Smoke compounds significantly worsened pancreatic necroinflammation and fibrosis in a rat model of AP. Ethanol and smoke compounds significantly increased PSC migration and ER stress. The inductive effects of ethanol and smoking on PSC proliferation were inhibited by the nAChR antagonist mecamylmine, suggesting that nAChRs may mediate PSC responses to smoke compounds. Smoking-related acceleration of alcoholic pancreatitis may be mediated by activation of PSCs upon exposure to alcohol and smoke compounds.

Figure 1 Results of the animal model

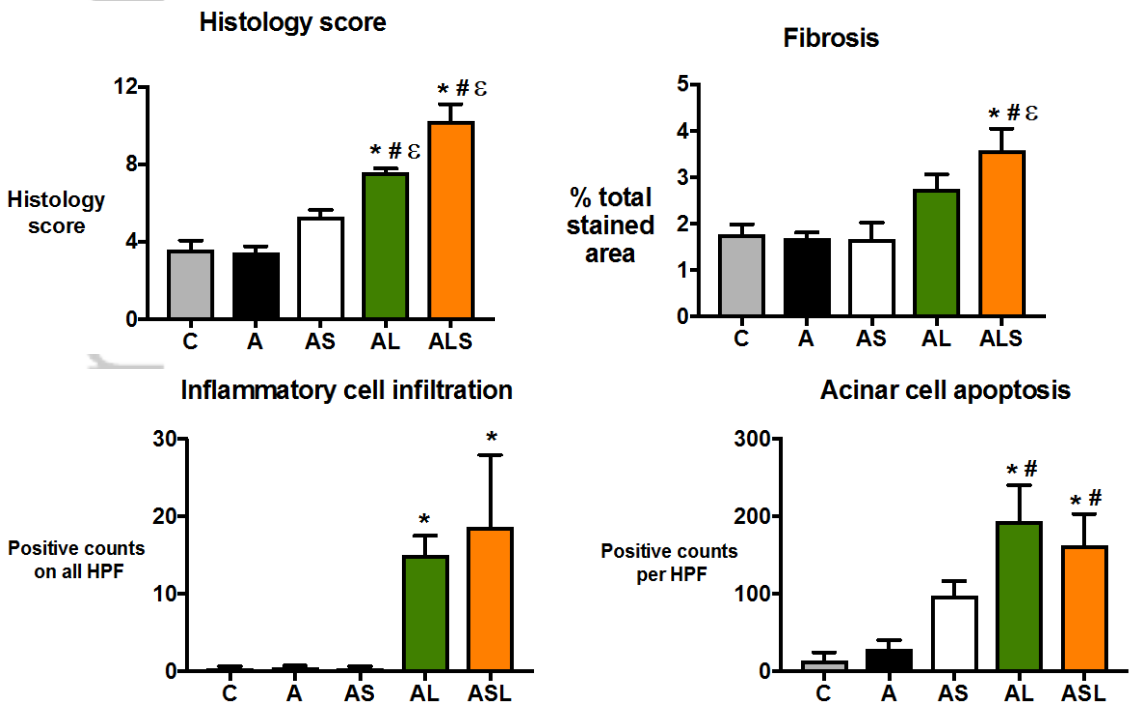

$n = 3$ rats/group. *$P < 0.05$ *vs* C, $^{\#}P < 0.05$ *vs* A, $^{\varepsilon}P < 0.05$ *vs* AS.